EVALUATION OF THE SHORT-TERM PERIODICITIES IN THE FLARE INDEX BETWEEN THE YEARS 1966–2002

ATİLA ÖZGÜÇ[1], TAMER ATAÇ[1] and JÁN RYBÁK[2]
[1]*Kandilli Observatory and E.R.I. Boğaziçi University, Çengelköy, Istanbul, Turkey*
(e-mails: ozguc@boun.edu.tr/atac@boun.edu.tr)
[2]*Astronomical Institute, Slovak Academy of Sciences, 05960 Tatranská Lomnica, Slovak Republic*
(e-mail: choc@astro.sk)

(Received 1 March 2004; accepted 4 June 2004)

Abstract. The short-term periodicities of the flare index are investigated in detail using Fourier and wavelet transforms for the full disc and for the northern and the southern hemispheres of the Sun separately over the epoch of almost 4 cycles (1966–2002). The most pronounced power peaks were found by the Fourier transform to be present at 25.6, 27.0, 30.2, and 33.8 days. The wavelet transform results show that the occurrence of periodicities of flare index power is highly intermittent in time. A comparison of the results of the Fourier transform and the time-period wavelet transform of the flare index time series has clarified the importance of different periodicities, whether they are or are not the harmonics of the basic ones, as well as the temporal location of their occurrence. We found that the modulation of the flare index due to the 27-day solar rotation is more pronounced during the declining portion of solar cycle than during the rising portion.

1. Introduction

The periodic variation of solar activity has been studied extensively since the discovery of solar rotation and the 11-year periodicity. Long-term variations of some solar activity indices are discussed in detail and spectral analysis updated in recent publications (see, e.g., Le and Wang, 2003; Özgüç, Ataç, and Rybák, 2002b).

Relatively recently, periodicities in the intermediate-term have been explored, starting with the discovery of a 153-day periodicity in γ-ray flare occurrence (Rieger *et al.*, 1984). Since then, many researchers have investigated these periodicities, using various solar activity indicators (see, e.g., for X-ray flares, Dennis, 1985; Bai and Sturrock, 1987; for flares producing energetic interplanetary electrons, Dröge *et al.*, 1990; for type II and IV radio bursts, Verma *et al.*, 1991; for microwave peak flux, Bogard and Bai, 1985; for flare index, Özgüç and Ataç, 1989, 1994; Özgüç, Ataç, and Rybák, 2002a; for sunspot area, Lean and Brueckner, 1989; Oliver, Ballester, and Baudin, 1998; and for sunspot numbers, Ballester, Oliver, and Baudin, 1999).

For short terms, the Sun often exhibits 27- and 13.5-day periodicities, which tell more about the spatial organization of the solar activity than its temporal organization. The origin of such quasi periodicities that are particularly prominent during solar maxima has remained a mystery for nearly two decades. The 13.5-day

Solar Physics **223:** 287–304, 2004.

periodicity, often seen, was first identified by Ward and Shapiro (1962) in sunspot numbers and several other measures of solar activity. Since the 27-day period is periodic but non-sinusoidal, the 13.5-day period could be its second harmonic. However, a detailed analysis by Donnelly and Puga (1990) showed that a 13- to 14-day periodicity was uniformly strong in the 1750–2900 Å range and was not simply a phase related second harmonic of a non-sinusoidal 27-day variation but was instead predominantly due to episodes of activity with two temporal peaks per rotation from groups of active regions roughly 180 deg apart in solar longitude. Recently Kane, Vats, and Sawant (2001) have also studied short-term periodicities in the solar emissions at different solar altitudes.

The presence of the long- and intermediate-term periodicities in flare index (FI) has been analyzed before for the cycles 20, 21, 22, and the rising part of cycle 23 (Özgüç, Ataç, and Rybák, 2003a), as well as for individual cycles by Özgüç and Ataç (1989, 1994) and Özgüç, Ataç, and Rybák (2002a). But this time we have considered only the short-term periodicities of the FI for the time period data from 1 January 1966 to 1 September 2002 which covers almost 36.5 years. Long-term observations of solar activity indicate that each hemisphere's solar activity is obviously statistically different from that of the other. Therefore both hemispheres and total surface of the Sun are examined separately to confirm the existence of solar activity periodicities.

To estimate periodicities the discrete Fourier transform (FT) was employed for the whole FI data used in this paper. Since the commonly used FT is not able to disclose the possible changes in the periodicities over the period studied, the wavelet transform (WT) was applied to search for temporal variability. In Section 2 we specify the data used and describe the methods of analysis. Results and discussion are given in Sections 3 and 4, respectively. However, first results on the short-term periodicities of the FI for the full disc have already been published (Özgüç, Ataç, and Rybák, 2003b).

2. Data and Methods of Analysis

2.1. Solar flare index

Solar activity can be measured at various heights in the solar atmosphere and these measurements can be compared with observed changes in the heliosphere. In this paper, we have considered the FI for the period data from 1 January 1966 to 1 September 2002 (total 13 392 days). The quantitative flare index, first introduced by Kleczek (1952), $Q = i\ t$, may be roughly proportional to the total energy emitted by the flare. In this relation, i represents the intensity scale of importance of a flare in Hα and t the duration in Hα (in minutes) of the flare. The determination of Q has been explained previously (Özgüç, Ataç, and Rybák, 2003a). Calculated

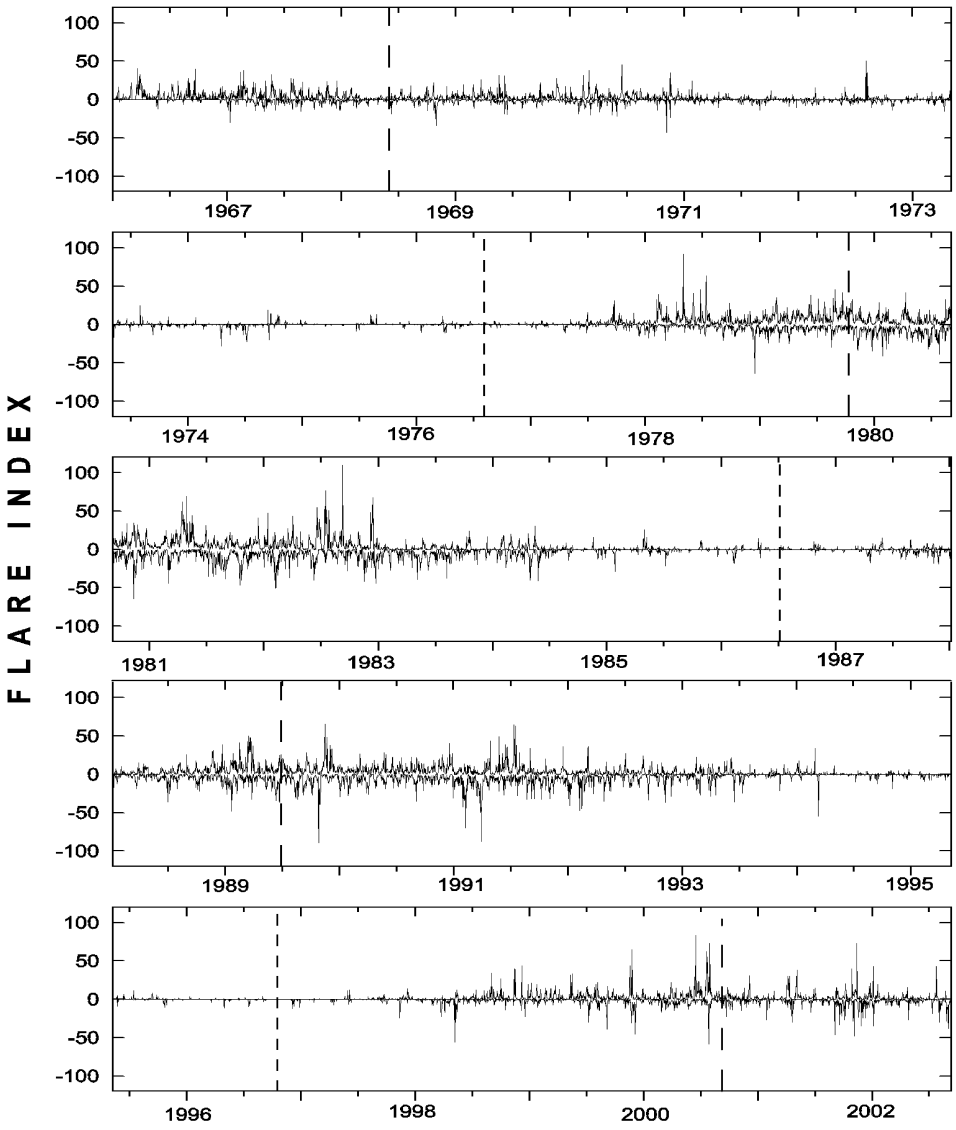

Figure 1. Behavior of the northern and the southern hemispheric FI daily values for the cycles 20 –22 and first half of cycle 23. The southern hemispheric FI values are denoted as minus to show them better. *Long-* and *short-dashed* vertical lines mark the solar activity cycle maxima and minima, according to NOAA mean monthly sunspot numbers, respectively.

values are available for general use in anonymous ftp servers of our observatory[1] and NGDC[2].

[1] ftp://ftp.koeri.boun.edu.tr/pub/astronomy/flare_index

[2] ftp://ftp.ngdc.noaa.gov/STP/SOLAR_DATA /SOLAR_FLARES/INDEX

This data set constitutes almost 36.5 years (see Figure 1). The flare index is an interesting parameter and is of value as a measure of the short-lived activity on the Sun and allows us to study long- and short-term variation of the Sun. Obtained results (e.g., Mavromichalaki *et al.*, 2003; Li *et al.*, 2002; Kane, 2002) have shown that the FI data set may be used to study solar activity and its relation with the other activity indicators as well as the heliospheric changes. Therefore this two dimensional index is physically good enough to describe the flare activity because there are no limitations to compile it. Recently, Caballero and Valdés-Galicia (2001) reported that as for the case of sunspots, the solar FI data are stationary.

2.2. Discrete Fourier transform

The search for periodicities in all the time series was performed by calculating the discrete Fourier transform. This technique provides which periodicities are in operation during the studied period, which covers about 13 392 days. We examined three FI time series, which are for the full-disc and for the northern and the southern hemispheres, by computing the periodograms after tapering 5% of the data at the ends of the time intervals by applying a split bell cosine window (Bloomfield, 1976).

Before computing the periodograms the means are subtracted from the time series; then they are divided by their standard deviations. However, daily flare occurrences are not statistically independent. If flare activity is high on a certain day, we can expect flare activity to be high for the next several days. By taking the weekly flare index as a time series, we avoid this problem.

The obtained power distribution should follow an exponential distribution (Horne and Baliunas, 1986); i.e., the probability of the power density at a given frequency being greater than k by chance is given by

$$P(z > k) = \exp(-k/\sigma^2), \tag{1}$$

where the normalization factor k should be determined empirically (Delache, Laclare, and Sadsaoud, 1985; Bai and Cliver, 1990; Bai, 1992). Even if we use a normalized time series

$$X_{ii} = (X_i - X_{av})/\sigma,$$

where X_i is the Q value on the ith day, X_{av} is the daily mean flare index value, and σ is the standard deviation, because of the interdependence of occurrence of some big flares, the Fourier periodogram turns out not to be normalized. Therefore, whatever analysis method is used, the best way to normalize the power spectrum is to fit the actual power distribution to Equation (1) (Bai and Cliver, 1990). Figures 2–4 top panels show the normalized power spectra of the three time series for the period intervals of 15–40 days. For these panels the power spectra were calculated for the 289–771 nHz range with 0.24 nHz interval. The uncertainty in each frequency is ± 0.4 nHz due to the 36.5-year data length. There are several

TABLE I

Periodicities found by Fourier power spectral analysis. P, F, and R show periods given in day, the FAP values, and the probability values after randomization of time series, respectively.

full-disc			Northern hem.			Southern hem.		
P	F(%)	R(%)	P	F(%)	R(%)	P	F(%)	R(%)
25.6	4.7	6.3	–	–	–	–	–	–
27.0	0.24	1.2	27.0	4.9	3.3	27.5	4.7	5.5
30.2	5.0	6.8	–	–	–	–	–	–
–	–	–	–	–	–	33.8	10.1	7.8

significant peaks in these figures whose statistical significances and probabilities of the obtained high peaks are listed in Table I. Figure 2 lower panel shows the distribution of the Fourier power values corresponding to the normalized spectra shown in the same figure but at top panel. The vertical axis shows the cumulative number of frequencies for which the power exceeds a certain value; of course for all frequencies the power exceeds zero. At only one or two frequencies the powers were their maximum values. For lower values of power, the distributions can be well fitted by the equations which are shown in Figure 2 (lower panel), as expected from Equation (1). Thus, we normalize the power spectrum by dividing the powers by these k factors to obtain Figure 2 top panel.

Once the power spectra have been properly normalized (which means that the constant k in Equation (1) has been computed for each spectrum and the power spectra divided by k) one has to evaluate the probability that a peak (with a normalized power) in the spectrum is due to chance. According to Scargle (1982) and Horne and Baliunas (1986) the false alarm probability (FAP) is given by

$$F = 1 - [1 - \exp(-Z_m)]^N, \tag{2}$$

where Z_m is the height of the peak in the normalized power spectrum and N is the number of independent frequencies. If we have a discrete power spectrum giving the power at each of N independent frequencies for a set of random data, then F indicates the probability that the power at one or more of these frequencies will exceed Z_m by chance.

Fourier components calculated at frequencies at intervals of the independent Fourier spacing (ifs), $\Delta f_{ifs} = \tau^{-1}$, where τ is the time span of the data, are totally independent (Scargle, 1982). For $\tau = 13\,392/7 = 1913.1$ days (since we studied with the weekly values) $\Delta f_{ifs} = 6.0$ nHz. Thus, there are 80 independent frequencies in the 289–771 nHz intervals. The FAP is calculated for each peak as follows: if we take the height of the peak and the number of independent frequencies (80) in Figure 2 for the full-disc, and substitute them in the FAP's expression,

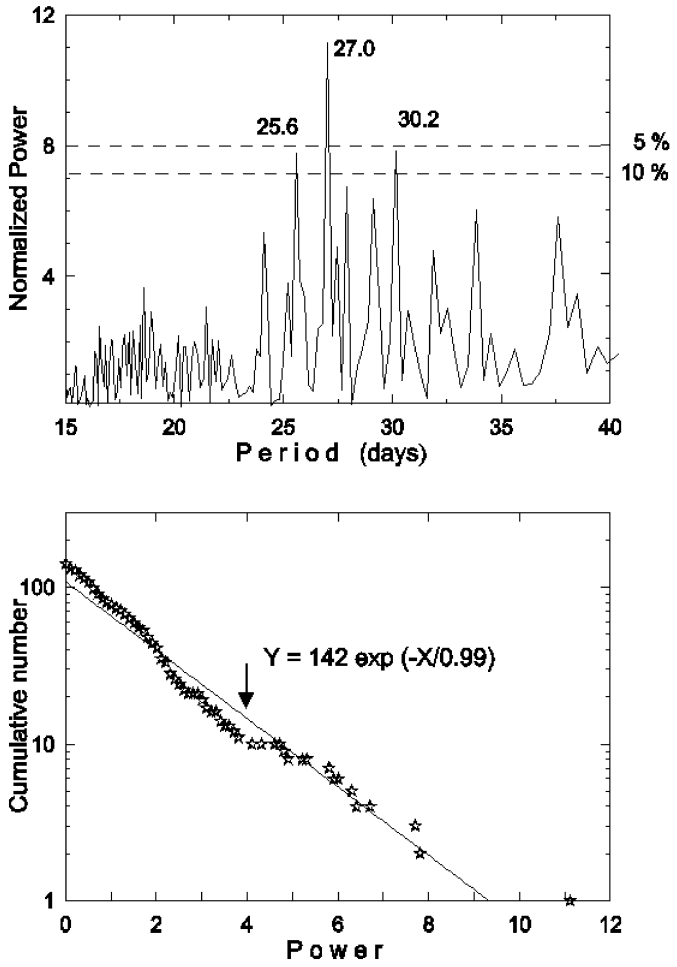

Figure 2. Normalized power spectra of the flare index (*top*) and power distribution of discrete Fourier transform (*lower*) of the full disc of the Sun for time interval of 13 392 days and for period interval of 15–40 days. The *dashed lines* at the top panel indicate the FAP significance levels. The *vertical axis* of the lower panel are the numbers of frequencies for which power exceeds X. The *straight line* is the fit to the points for lower values of power.

we would underestimate the FAP (in our case we would obtain 0.13%). However, when substituting $N = 142$ we compensate for the effect of the increase of the peak value by oversampling. The oversampling tends to more accurately estimate the peak value. Therefore, if we substitute $Z_m = 11.0$ and $N = 142$ (since we searched 142 frequencies with 3.4 nHz intervals) in Equation (2) we get the false alarm probability $F = 0.0024$; i.e., the probability to obtain such a high peak by chance is about 0.24%. The same analysis has been applied to the corresponding time series and the results can be seen in Table I.

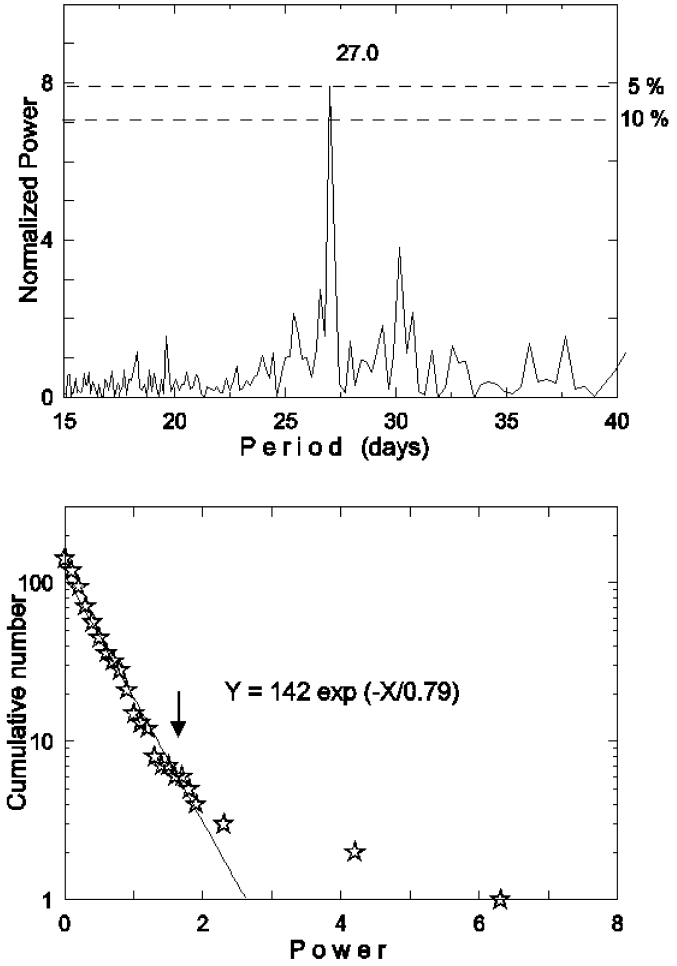

Figure 3. Same as Figure 2, but for the northern hemisphere.

Since peaks in a periodogram may arise from aliasing or other phenomena not present in Gaussian noise (e.g., spectral leakage arising from the spacing of the data and from the finite length of the time series), the FAP criterion, alone, is insufficient for establishing whether or not a strong peak in a periodogram is indeed a real periodicity in the time series. Also, some small peaks present in the original periodogram can be real in the case when the normalized factor k would be too large in consequence of treating real periods as noise. We test for genuine peaks by recomputing the periodogram after randomizing the data on the time grid. This procedure (Delache, Laclare, and Sadsaoud, 1985; Özgüç, Ataç, and Rybák, 2002a) maintains the noise characteristics of the time series but destroys all coherent signals, especially those with periods longer than the chosen cut interval of the data. In our time series, we cut the data with a fifteen-day interval and then shuffle

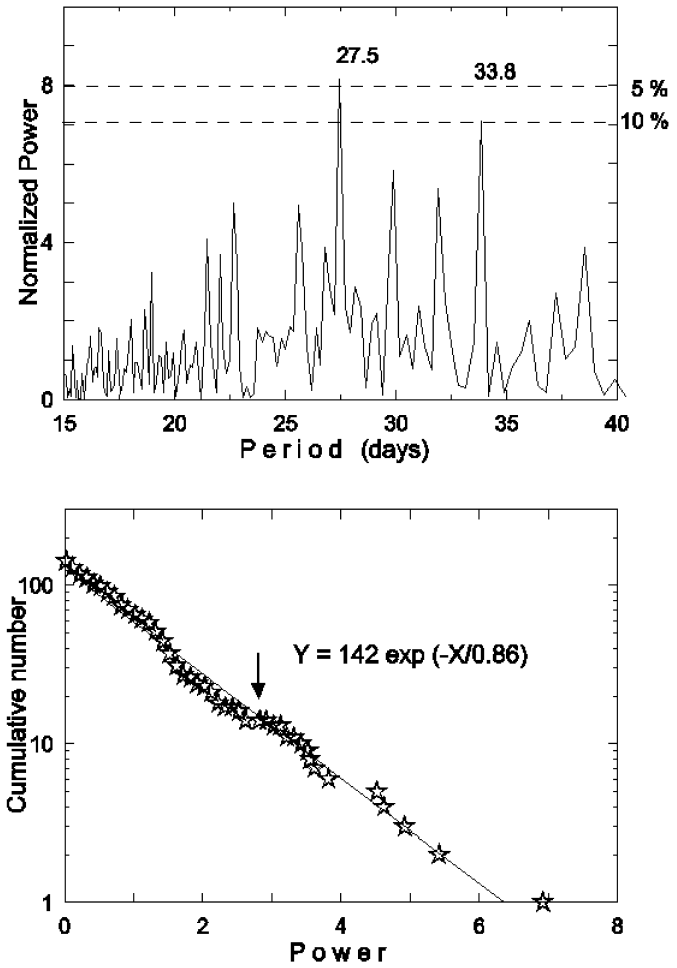

Figure 4. Same as Figure 2, but for the southern hemisphere.

them to obtain a randomized data set. Then we calculate the power of the randomized data set at the number of independent frequencies in the selected frequency interval, which we searched. We repeat these simulations 1000 times for each time series, every time computing the number of cases in which the recalculated power values for the periods having peaks in the original spectrum equal to or larger than the peaks power of the real data. The results of these calculations are presented in Table I. After inspection of this table, the results of these analyses give us confidence that the peaks in Figures 2–4 arise from coherent signals. Although there are some differences between FAP and randomizing test results, they may arise from the selected randomizing method, which yields insufficient randomizing in some cases.

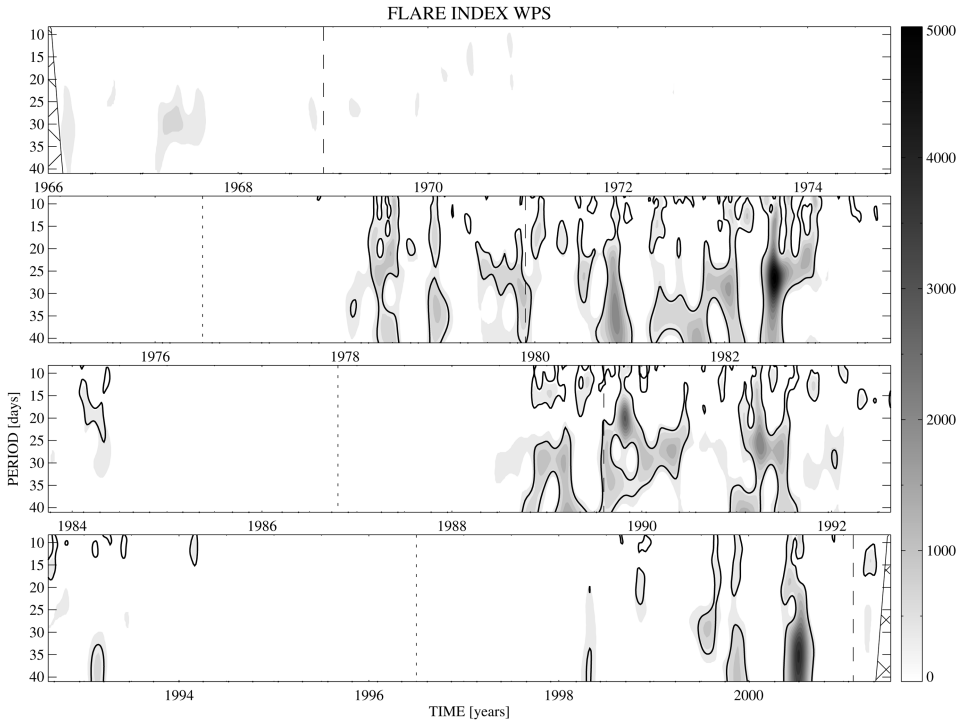

Figure 5. The wavelet power spectra of the FI time series for the whole surface of the Sun for the period range 8–40 days. Grey-scale coding of power from white to black represents the square root of power (a. u.) in a linear scale given on the right side bar. The *solid curve* shows the 95% confidence levels of the local power above the noise level assuming noise independence on periods. The cone of influence is marked by the cross-hatched regions. *Dashed* and *dotted vertical lines* mark the solar activity cycle maxima and minima according to the Wolf's sunspot index, respectively.

2.3. WAVELET ANALYSIS

The wavelet transform (WT) analysis yields information on periodicities of the studied signal in both time and frequency domains (e.g., Daubechies, 1990; Kumar and Faufoula-Georgiou, 1997). Therefore we have also applied wavelet analysis to the time series of FI to study the temporal variation of periodicities. These three time series were smoothed with 7-day running means before the WT calculations. Algorithm of the continuous wavelet transform was applied within the period range 8–41 days (Torrence and Compo, 1998). The Morlet wavelet, a plane sine wave with an amplitude windowed in time by a Gaussian function, has been selected to search for variability of the time series of daily FI data. The used period resolution varied from 0.18 to 1.42 days. The calculated wavelet power is suppressed on the edges of the time domain due to the applied WT algorithm within the cones of influence located at the temporal edges of the domain (indicated in our plots by cross-hatched regions).

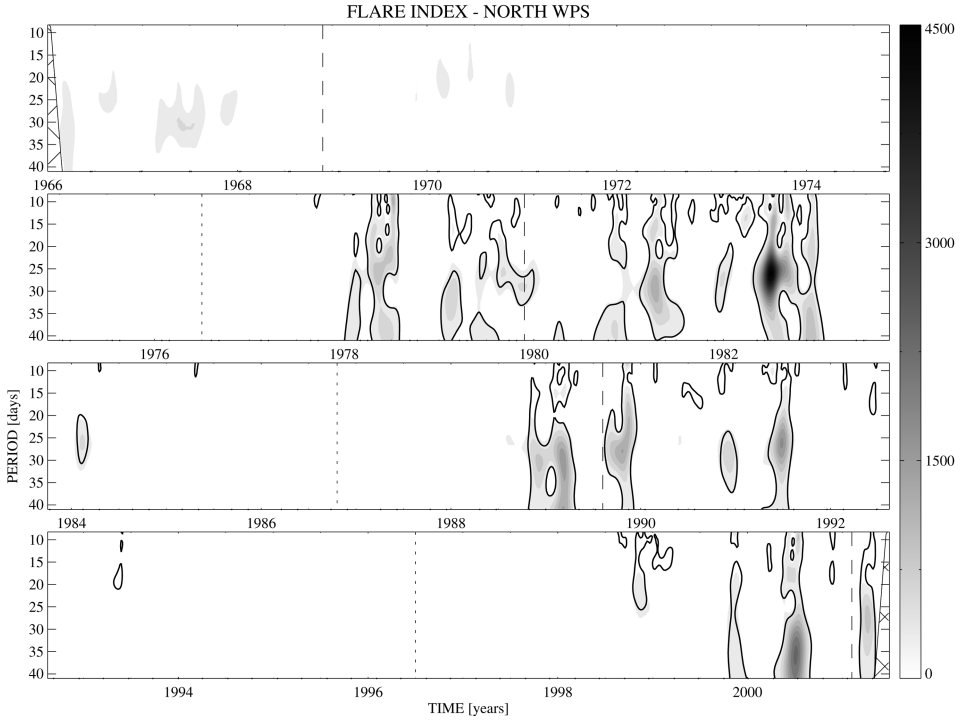

Figure 6. The wavelet power spectra of the FI time series for the northern hemisphere of the Sun for the period range 8–40 days. Details are as Figure 5.

The non-dimensional frequency has been set to 6 fixing the length of all wavelets according to their scale. The significance level of the calculated WT power was derived using the null hypothesis assuming existence of the global power spectrum (Torrence and Compo, 1998). The 95% confidence level, used in this study, implies that 5% of the wavelet power should be above this level for each period. Following this way the plots of 3 wavelet power spectra (WPS) were prepared for data series of FI on the northern and the southern hemispheres as well as on the full-disc of the Sun (Figures 5–7).

3. Results

In this work we tried to show the temporal variations of the flare index over the years, which we studied around the rotation period. The Fourier transform and the wavelet techniques are utilized to study the time variation of power spectra for a selected period interval of 15–40 days (for WT 8–40 days), since the wavelet transform method gives detailed information on the time localization of each periodicity.

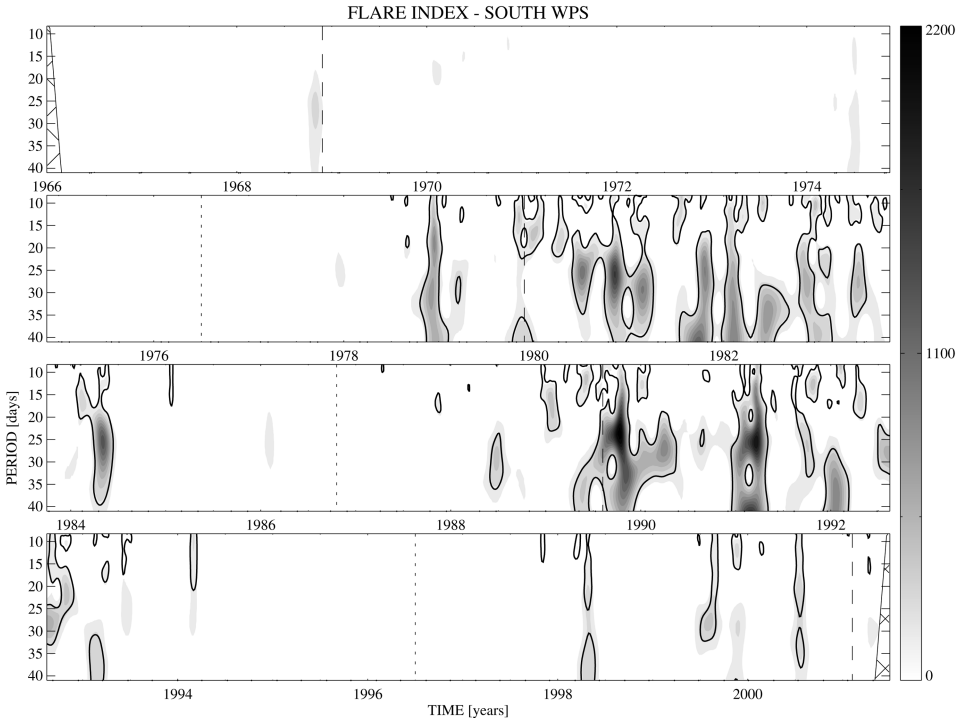

Figure 7. The wavelet power spectra of the FI time series for the southern hemisphere of the Sun for the period range 8–40 days. Details are as Figure 5.

Figures 2–4 show the normalized power spectra (amplitudes versus periodicities) of the time series of the FI for the period interval of 15–40 days. For these figures the power spectra were calculated for the 289–771 nHz range with 3.4 nHz intervals. There are several significant peaks in this figure whose statistical significances are high.

The most prominent period is the 27.0-day peak in the power spectrum of FI for the total surface of the Sun. The second one is the 25.6 days peak whose significance is about 5% FAP level (Figure 2); and the third one is the 30.2 days peak with the same significance as the latter. Although these three peaks seem very close to each other, they are farther than the uncertainty value of 0.4 nHz from each other; so we can say that they are not overlapped with one another. The northern hemisphere time series of FI gives only one prominent period, which is 27.0 days (Figure 3) with a high enough significance level. A close look at Figure 4 which illustrates the southern hemisphere time series of FI, shows two peaks which reach above 10% FAP level; these are 27.5 days and 33.8 days periodicities. The rest of the peaks are below the 10% FAP level.

Remarkable are some differences of the power spectra between the total and hemispheric FI. One could expect that the power spectrum of the total index will be the simple sum of power spectra of both hemisphere. Nevertheless, different

phases of each period under study at each hemisphere can lead to a completely different situation when, e.g., very weak peak in the northern hemisphere and the broad weak peak in the southern hemisphere, both close to 30.2 days, generate a significant peak for the FI of the full disc. Contrary to the previous one, the 33.8-day period has a weak peak in the full disc of FI and no peak in the northern hemisphere but it has a significant peak in the southern hemisphere. All periods found well above the given statistical levels are therefore real although this strange relation between the separate behavior of power at separate hemispheres according to the total index can be found.

The short-term period WT power spectra are displayed in Figures 5–7 for the full disc, northern and southern hemispheres, respectively. The time–period distributions of the these WPS show extremely intermittent behavior of power at all periods. All three FI series show that the major periods, obtained by Fourier transform are localized in short time intervals (typically up to half of a year). Generally the pulses of power are very short in time. This fact is complementary to the relatively large number of individual periods of less significant power derived for all three FI series by FT (Figures 2–4). All significant FT short periods (Table I) can be identified during some temporal moments of the series where corresponding pulses of WT power are found (e.g., for the full-disc FI the 27.0, 25.6, and 30.2 days periods are localized in years 1982.5, 1991.2, and 1989.1, respectively). Moreover, when searching for other (less significant) FT periods in the WT power spectra adequate pulses of power can be found as well, e.g., for the full-disc FI pulses of WT power for 33.8 and 37.5 days periods are positioned at 1979.0 and 2000.5 year, respectively.

Occurrence of power is predominant on the ascending or descending phase of the solar cycles and pulses of power are distributed within large temporal intervals starting 1–2 years after the solar cycle minimum finishing 2–3 years before the next minimum. The cycle 21 is an exception from this rule as the amplitude is significantly lower in all pulses of WT power here and none of them reach the selected significance level. The same is valid also for the epochs of solar cycle minima where the FI values are generally much lower then in other parts of solar cycle.

Some of the pulses of power are well isolated within the WT power spectra (e.g., southern hemispheric FI in year 1984) and some other pulses cover wider range of periods while still localized to a short temporal interval (e.g., beginning of year 1979 in the same series). Comparing the actual length of the daughter wavelets used for calculation of WT $6\times(8-40)$ days $= 48-240$ days to duration of the individual pulses of power in the WT power spectra we see that the regular periodicities of the FI series have to be usually even shorter than the length of the used wavelets for the particular period range under study.

Moreover significant differences are clearly visible in the WT power spectra of the hemispheres and/or of the full disc. Let us notice two illustrative examples of flare activity pronounced solely at one hemisphere: the southern hemispheric FI

at 1992.5 and at about 27 days period and the northern hemispheric FI at 1982.6 and at 27.5 days period. The two pulses have no counterpart on the supplementary hemisphere. Then the full-disc FI, which is a sum of two hemispheric ones, leads to an averaging information masking the independent behaviour of flare activity and its periodicities on the northern and southern hemispheres.

4. Discussion

To understand any periodic variation in solar activity records that may be indicative of true solar cyclicity, there is a practical need to characterize quantitatively those sources of variance that are potential tools for predicting future solar activity. Therefore, we have studied temporal variations of the flare index considering the FI for the period 1966–2002. We examined, in the FI data, the reality of solar periodicities concentrating on periods between 8 and 40 days. During this time period, FI shows some periodicities listed in Table I.

4.1. Consistency with the earlier results

The fundamental period proposed by Bai and Sturrock (1993) was reported as 25.5-day. In our analysis, we found this value as 25.6 days. However, Zieba *et al.* (2001) found the rotation rate of the 'active longitudes' in the rising phase of cycle 23 as equal to 26.0 ± 0.3 days. They supposed that this period can be identified with a fundamental period of an unknown Sun's clock as a lot of the known periodicities are subharmonics of it. Recently, Bai (2003a) studied longitude distributions of major flares in a coordinate system rotating about the solar axis, using the rotation period as a free parameter. And he concluded that, the idea of 25.5 days is a fundamental period of the Sun is well supported by data. The differences between the results of the different authors can be explain that because of the non-sinusoidal nature of the variation of some activities (e.g., square waveform shape of an X-ray source), a broad fundamental frequency will appear in the power spectra (Bouwer, Pap, and Donnelly, 1990). However, its clock mechanism is still unknown.

Using the flare occurrence rates between the cycles 19–23 Bai (2003b) found a 33.5 day periodicity. He reported that amplitudes of modulation tend to increase with increasing peak X-ray fluxes; and he added that such a trend is shown most strongly in this periodicity. In our analysis we found this periodicity as 33.8-day only in the southern hemisphere with an adequate significance level.

Some periods seen in the other activity indices may not be detected in the FI; however, recently, Rybák and Dorotovic (2002) have found a significant coronal index variability particularly for a period of 28 days in the time period of 1947–1998 which covers part of ours. In our analysis we could find no evidence neither for this period nor for the period of 35-day which was reported by Caballero and Valdés-Galicia (2001) for the sunspot number and hard X-ray flux for the time

interval 1990 and 1999. However, Lou *et al.* (2003) have found 35.85 days and 33.49 days periodicities by using coronal mass ejections (CMEs) and 38.71 and 33.53 days periodicities by using X-ray flares $\geq$ M 5.0 during the most recent solar maximum in cycle 23. 33.53 and 33.85 days periodicities are very close to our finding of 33.8 days but the two others are not seen in our analysis.

Ballester, Oliver, and Baudin (1999) put forward a hypothesis sustaining that when the periodicity appears in sunspots areas only, i.e., when the magnetic flux emerges mostly within already formed active regions, a similar periodicity should appear in high-energy solar flares. To the contrary, when the periodic emergence of magnetic flux is produced in the form of new and scattered sunspot groups, no periodicity should appear in energetic solar flares due to the small magnetic complexity of sunspot groups.

4.2. TEMPORAL APPEARANCE OF THE SHORT PERIODS

Before any interpretation of the pulses of power derived by the WT it is worth to analyse the extreme case of WT power pulses which are extended over almost the whole range of periods under study. Illustrative example found in the southern FI series located at transition 1978/1979 showing a main peak of FI located at 1978.95 with several regularly spaced in time peaks of FI before it. These peaks seem to be caused by rotation of rather localised activity on the solar surface. On the other hand, after the main peak at 1978.95 almost 10 other weak peaks of similar height are localised within the temporal range 1979.0 and 1979.1. The used WT links the main peak with all other weak peaks producing power over the whole period range 10–40 days, but still localised to narrow time interval of 0.1–0.2 year.

Conversely, clear isolated pulses of power like that one of the southern hemispheric FI situated in the first half of the year 1984 are created by flare activity in one center of activity as it rotates around the Sun.

Determined temporal shifts of period in some of the pulses of power by the WT can be explained also on the above-mentioned example of the isolated pulses of power in the southern hemisphere in 1984. There are 3 weaker, but clearly shaped, peaks of FI data located at January 10, 18, and 23. The WT method recognised repetition of these peaks as periodicity seen in the power spectrum as a pulse of power around 16 days period at 1984.1. These FI peaks come from flare activity, localised in two active regions, which produced 3 short intervals of the enhanced flare activity.

It is worth stressing that WT allows to trace periodicities (or better said time intervals) of just a few pulses of flare activity. Thus the periodicities obtained cover not only information on rotation of active regions but possibly also information on longitudinal distances of active regions (if flaring activity is localised in few active regions sufficiently far away in longitudes and their flaring activity is constant) caused by rotation (rising/setting of active regions); information on temporal vari-

ation of flaring activity as the AR passes the solar disc (14 days); and possible combination/interference of these effects.

Investigation of pulses of power in the WT power spectra should be accompanied by checking of the particular parts of the FI data series in order to reveal reasons for occurence of the particular pulse.

4.3. PHYSICAL IMPLICATIONS OF THE SHORT PERIODS

Periodicities very near 27 days are easily attributable to an effect of solar rotation. Slight variations could occur if the active region had a slow longitudinal movement ahead of, or lagging behind the rotation. This is a possibility.

Our results show that 27-day modulation seems to be 27.5-day in the southern hemisphere of the Sun. There is a possibility that some parts of an active region move rapidly forward or backward with respect to the mean rotation rate of the Sun, to give spacings different from 27 days. This can be checked only by an actual image comparison.

We found that the modulation of the flare index due to the 27-day solar rotation is more pronounced during the declining portion of solar cycle than during the rising portion. The earlier conclusion of Pap, Tobiska, and Bouwer (1990) that this arises because active regions and their magnetic fields are better organized and more long-lived during the maximum and declining portion of solar cycle than during its rising portion.

The WT of FI confirms that these periodicities are intermittent. This fact is so pronounced that besides an explanation of different periodicities, also the natural reason for the intermittence has to be found as well. Recently the existence of equatorially trapped large-scale Rossby type waves (Rossby, 1939) have been proposed as the physical origin of such quasi periods by Lou *et al.* (2003). They proposed that the photospheric magnetic flux emergence might be modulated by equatorially trapped Rossby-type waves. Hence a dynamic feedback cycle may be established to sustain quasi-periodicities in magnetic flux emergence and flare activities. However, powerful solar flares and CMEs frequently occur in magnetically active regions. As a solar flare or a CME goes off, a fraction of their energy will back-react on the solar photosphere and appear in the form of travelling disturbances. To sustain such a 'dynamic feedback cycle' initiations and positive feedbacks above a certain 'energetic threshold' are necessary. This may explain why Rieger-type periodicities in the emergence of magnetic flux, sunspot areas and high energy flares, etc., are detected within a few years around the solar maxima when solar activity levels are high. This also implies a possible change in the most dominant periodicities with different physical conditions for different solar maxima. After analyzing the FI time series, we find that episodes of the 27-day periodicity occurred after the maxima of cycles. The wavelet power of this oscillation peaks around the middle of the declining phase of cycles 21 and 22, with the magnitude of peak values changing from one cycle to the next. These episodes

may be useful for a theoretical understanding of these kind of periodicities since it was long overdue.

However, Ruzmaikin (2001) brings another explanation that the magnetic fields emerge at the solar surface at random times and place when the total magnetic field (mean field plus a fluctuation) exceeds the threshold for buoyancy. In this way the mean field is responsible for the observed regularities of the sunspot magnetic fields, such as the Hale's law and the 11-year periodicity, and the fluctuating fields are responsible for emergence of individual flux tubes then merging into sunspots.

Recently Schatten (2003) brings a new interpretation to the Babcock dynamo. In this model the Sun's polar fields near solar minimum are wrapped up by differential rotation to form the toroidal fields, which later float to the Sun's surface and erupt to form active regions where active flares are formed. Hence over an 11-year solar cycle the amplification sometimes regenerates more polar field and sometimes less. At the same time Hathaway *et al.* (2003) have reported strong observational evidence that a deep meridional flow toward the equator is driving the sunspot cycle. Obviously, other mechanisms such as fluctuations in the meridional flow (Hathaway, 1996) believed to be a product of turbulent convection and variations in the gradient of the rotations rate also contribute to the cycle amplitude variations. The differences of the speed of the meridional circulation during cycles with different amplitudes and all the mechanisms mentioned above can act as an intrinsic dynamics which sets the short-term variations in the period of cycle. We can expect that the meridional circulation can be a time keeper or a solar clock for the time variations of the solar cycles.

5. Conclusion

Our study as well as many previous studies by a number of authors have resulted in a wide range of solar periodicities and of the intermittent behaviours, which are not easy to explain. This indicates that the problem of solar periodicities is still open and needs new observational data. Therefore, the solution of the observed solar periodicities should be sought in a complicated Sun's magnetic system which generates in the different solar data the compound set of solar periodicities.

Acknowledgements

The wavelet transform algorithm of C. Torrence and G. P. Compo, available at *http://paos.colorado.edu/ research/wavelets/* has been used in this work. This work was supported by Boğaziçi University Research Fund by the project of 00T101 and by the Slovak grant agency VEGA by the grant 2/3015/23. This research is part of the European Solar Magnetism Network (EC/RTN contract HPRN-CT-2002-00313).

References

Bai, T.: 1992, *Astrophys. J.* **397**, 584.
Bai, T.: 2003a, *Astrophys. J.* **585**, 1114.
Bai, T.: 2003b, *Astrophys. J.* **591**, 406.
Bai, T. and Cliver, E. W.: 1990, *Astrophys. J.* **363**, 299.
Bai, T. and Sturrock, P. A.: 1987, *Nature* **327**, 601.
Bai, T. and Sturrock, P. A.: 1993, *Astrophys. J.* **409**, 476.
Ballester, J. L., Oliver, R., and Baudin, F.: 1999, *Astrophys. J.* **522**, L153.
Bloomfield, P.: 1976, *Fourier Analysis of Time Series: An Introduction*, John Wiley and Sons, New York.
Bogard, R. S. and Bai, T.: 1985, *Astrophys. J.* **229**, L51.
Bouwer, S. D., Pap, J., and Donnelly, R. F.: 1990, in K. H. Schatten and A. Arking (eds.), *Climate Impact of Solar Variability, NASA Conf. Proc. 3086*, NASA, Greenbelt, MD, p. 125.
Caballero, R. and Valdés-Galicia, J. F.: 2001, *Adv. Space Res.* **27**, 583.
Daubechies, I.: 1990, *IEEE Transactions on Information Theory* **36**, 961.
Delache, P., Laclare, F., and Sadsaoud, H.: 1985, *Nature* **317**, 416.
Dennis, B. R.: 1985, *Solar Phys.* **100**, 465.
Donnelly, R. F. and Puga, L. C.: 1990, *Solar Phys.* **130**, 369.
Dröge, W., Gibbs, K., Grunsfeld, J. M., Meyer, P., and Newport, B. J.: 1990, *Astrophys. J. Suppl.* **73**, 297.
Hathaway, D. H.: 1996, *Astrophys. J.* **460**, 1027.
Hathaway, D. H., Dibyendu, N., Wilson, M. R., and Reichmann, E. J.: 2003, *Astrophys. J.* **589**, 665.
Horne, J. H. and Baliunas, S. L.: 1986, *Astrophys. J.* **302**, 757.
Kane, R. P.: 2002, *Solar Phys.* **207**, 17.
Kane, R. P., Vats, H. O., and Sawant, H. S.: 2001, *Solar Phys.* **201**, 181.
Kleczek, J.: 1952, *Publ. Inst. Centr. Astron.*, No. 22, Prague.
Kumar, P. and Faufoula-Georgiou, E.: 1997, *Rev. Geophysics* **35**, 385.
Le, G. M. and Wang, J. L.: 2003, *Chin. J. Astron. Astrophys.* **3**, 391.
Lean, J. and Brueckner, G. E.: 1989, *Astrophys. J.* **337**, 568.
Li, K. J., Wang, J. X., Xiong, S. Y., Liang, H. F., Yun, H. S., and Gu, X. M.: 2002, *Astron. Astrophys.* **383**, 648.
Lou, Y., Wang, Y., Fan, Z., Wang, S., and Wang, J. X.: 2003, *Monthly Notices Royal Astron. Soc.* **345**, 809.
Mavromichalaki, H. *et al.*: 2003, *J. Atmos. Solar. Terr. Phys.* **65**, 1021.
Oliver, R., Ballester, J. L., and Baudin, F.: 1998, *Nature* **394**, 552.
Özgüç, A. and Ataç, T.: 1989, *Solar Phys.* **123**, 357.
Özgüç, A. and Ataç, T.: 1994, *Solar Phys.* **150**, 339.
Özgüç, A., Ataç, T., and Rybák, J.: 2002a, *J. Geophys. Res.* **107**, 10.1029/ 2001JA009080.
Özgüç, A., Ataç, T., and Rybák, J.: 2002b, in A. Wilson (ed.), *Solar Variability: from Core to Outer Frontiers* **ESA SP-506**, 709.
Özgüç, A., Ataç, T., and Rybák, J.: 2003a, *Solar Phys.* **214**, 375.
Özgüç, A., Ataç, T., and Rybák, J.: 2003b, in A. Wilson (ed.), *Solar Variability as an Input to the Earth's Environments*, **ESA SP-535**, 687.
Pap, J., Tobiska, W. K., Bouwer, S. D.: 1990, *Solar Phys.* **129**, 165.
Rieger, E., Share, G. H., Forrest, D. J., Kanbach, G., Reppin, C., and Chupp, E. L.: 1984, *Nature* **312**, 623.
Rossby, C.-G.: 1939, *J. Marine Res.* **2**, 38.
Ruzmaikin, A.: 2001, *Space Sci. Rev.* **95**, 43.
Rybák, J. and Dorotovic, I.: 2002, *Solar Phys.* **205**, 177.
Scargle, J. D.: 1982, *Astrophys. J.* **263**, 835.

Schatten, K. H.: 2003, *Adv. Space Res*. **32**, 451.
Torrence, C. and Compo, G. P.: 1998, *Bul. American Meteor. Soc.* **79**, 61.
Verma, V. K., Joshi, G. C., Uddin, W., and Palival, D. C.: 1991, *Astron. Astrophys*. **90**, 83.
Ward, F. and Shapiro, R.: 1962, *J. Geophys. Res*. **67**, 541.
Zięba, S., Maslowski, J., Michalec, A., and Kulak, A.: 2001, *Astron. Astrophys*. **377**, 297.